Available online at www.sciencedirect.com
SCIENCE DIRECT®
Journal of Solid State Chemistry 179 (2006) 18–28
JOURNAL OF SOLID STATE CHEMISTRY
www.elsevier.com/locate/jssc

New process of preparation, X-ray characterisation, structure and vibrational studies of a solid solution $LiTiOAs_{1-x}P_xO_4$ ($0 \leqslant x \leqslant 1$)

M. Chakir[a,*], A. El Jazouli[a], J.P. Chaminade[b], F. Bouree[c], D. de Waal[d]

[a]*Laboratoire de Chimie des Matériaux Solides, Université Hassan II, Faculté des Sciences Ben M'Sik, Casablanca, Maroc*
[b]*Institut de Chimie de la Matière Condensée de Bordeaux, CNRS, 87, Av. Dr. Schweitzer, 33608 Pessac, France*
[c]*Laboratoire Léon Brillouin (CEA-CNRS), CEA/Saclay, 91191 Gif-sur-Yvette Cedex, France*
[d]*Department of Chemistry, University of Pretoria, 0002 Pretoria, South Africa*

Received 11 July 2005; received in revised form 22 September 2005; accepted 23 September 2005
Available online 2 November 2005

Abstract

$LiTiOAs_{1-x}P_xO_4$ ($0 \leqslant x \leqslant 1$) compounds have been prepared using solutions of Li, Ti, As and P elements as starting products. Selected compositions have been investigated by powder X-ray or neutrons diffraction analysis, Raman and infrared spectroscopy. The structure of $LiTiOAs_{1-x}P_xO_4$ ($x = 0$, 0.5 and 1) samples determined by Rietveld analysis is orthorhombic with *Pnma* space group. It is formed by a 3D network of TiO_6 octahedra and XO_4 ($X = As_{1-x}P_x$) tetrahedra where octahedral cavities are occupied by lithium atoms. TiO_6 octahedra are linked together by corners and form infinite chains along *a*-axis. Ti atoms are displaced from the centre of octahedral units in alternating short (1.700–1.709 Å) and long (2.301–2.275 Å) Ti–O bonds. Raman and infrared studies confirm the existence of Ti–O–Ti chains. Thermal stability of $LiTiOAsO_4$ has been reported.

Keywords: Structure; Powder diffraction; X-rays; Neutrons; Raman; Infrared

1. Introduction

Compounds belonging to the potassium titanyl phosphate $KTiOPO_4$ family have been extensively studied for their non-linear optical properties [1–10]. Recently, we have prepared and characterized new oxyphosphates of formula $M_{0.5}TiOPO_4$ (M = Ni, Co, …) [11,12], $Li_{(1-2x)}Ni_xTiOPO_4$ [13] and $Ni_{(1-x)}Cr_{(1-2x)}Ti_{2x}OPO_4$ [14]. Substitution of As for P leads to new oxyarsenates, which will be published elsewhere. The structure of $LiTiOPO_4$ has been determined from single crystal [10] and from powder X-ray diffraction data [3]. The structure of $LiTiOAsO_4$ prepared by solid state reaction has been reported by A. Robertson et al. [3]. However, the X-ray powder diffraction pattern published by these authors contains Li_3AsO_4, TiO_2 rutile and other phases. The present work reports on a new method of synthesis, crystal structure and vibrational spectra of $LiTiOAs_{1-x}P_xO_4$ ($0 \leqslant x \leqslant 1$) series. The thermal stability of $LiTiOAsO_4$ is also reported.

2. Experimental

$LiTiOAs_{1-x}P_xO_4$ ($0 \leqslant x \leqslant 1$) compounds have been prepared from aqueous solution of $(NH_4)H_2AsO_4$ (I), $(NH_4)_2HPO_4$ (II), Li_2CO_3 dissolved in dilute nitric acid solution (III) and solution of $TiCl_4$ diluted in ethanol (IV) as starting materials. The mixture (precipate + solution), obtained by slow addition of (IV) in (I + II + III) at room temperature, was dried at about 60 °C to remove the volatile compounds and heated progressively from 200 °C up to 600–800 °C with intermediate regrinding. The obtained final products were white. The thermal stability of $LiTiOAsO_4$ has been studied between 600 and 1000 °C.

*Corresponding author. Fax: (212) 22 70 46 75.
E-mail address: fachakir@yahoo.fr (M. Chakir).

0022-4596/$ - see front matter © 2005 Elsevier Inc. All rights reserved.
doi:10.1016/j.jssc.2005.09.047

X-ray diffraction data have been collected at room temperature on a Philips PW 3040 (θ–θ) diffractometer with the following experimental conditions: Bragg–Brentano geometry; diffracted-beam graphite monochromator; Cu$K\alpha$ radiation (40 KV, 40 mA); Soller slits of 0.02 rad on incident and diffracted beams; divergence slit of 1°; anti-scatter slit of 1°; receiving slit of 0.05 mm; holder surface corrected with a razor-blade; sample spinner used; steps of 0.02°(2θ) over the angular range 10°–120° (2θ) with a fixed counting time of 30 s.

Neutron diffraction data have been collected at room temperature on the high resolution powder diffractometer 3T2 in Saclay (LLB, Orphée Reactor), with: $\alpha_1 = 10'$; focusing (335) Ge monochromator; $\lambda = 1.2251$ Å; 6–125.70° angular range of measurement (2θ), 0.05° step; 20 He^3 detectors, $\alpha_3 = 10'$.

Raman spectra were recorded using a Dilor XY Raman microprobe. The samples were excited with the 514.5 nm line of an argon ion laser (Coherent model Innova 300). The spectral resolution was 3 cm^{-1}, the laser output power 110 mW, and the integration time 30 s. Infrared (IR) spectra were recorded on a Bruker IFS 113v FTIR spectrometer as KBr or polyethylene pellets. The spectra resolution was 2 cm^{-1}.

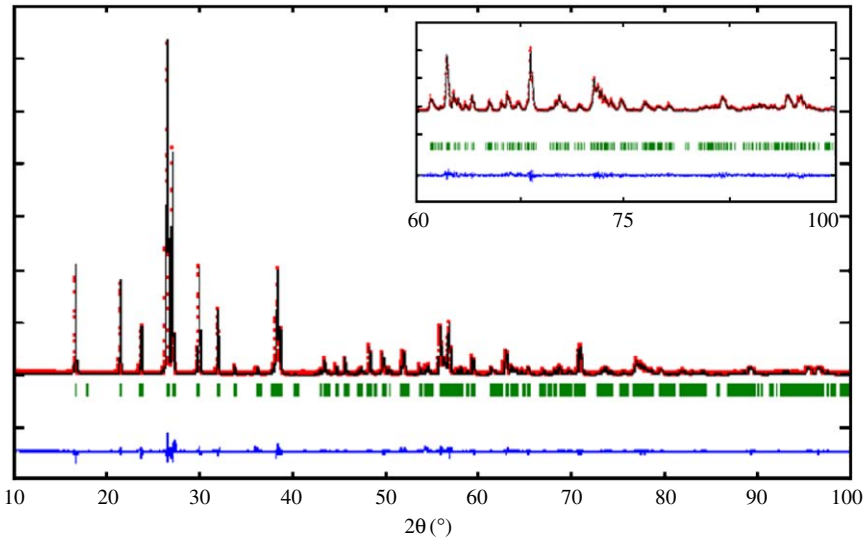

Fig. 1. Final observed (…), calculated (—) and difference X-ray profiles for $LiTiOAsO_4$.

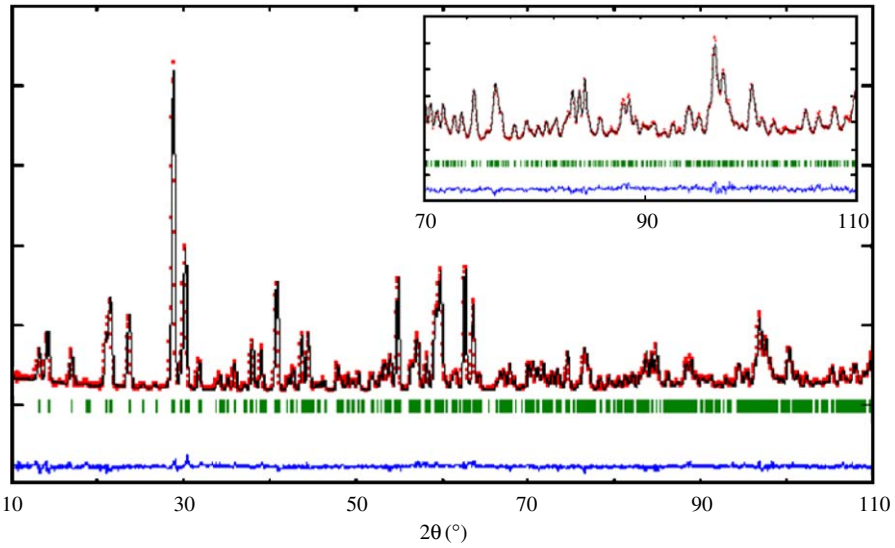

Fig. 2. Final observed (…), calculated (—) and difference neutrons profiles for $LiTiOAsO_4$.

Table 1
Refinement conditions (X-ray and neutrons (*) powder data) for $LiTiOAs_{1-x}P_xO_4$ ($x = 0$, 0.5 and 1)

	$LiTiOAsO_4$*	$LiTiOAsO_4$	$LiTiOAs_{0.5}P_{0.5}O_4$	$LiTiOPO_4$
Zero point (°, 2θ)	0.0172	0.0002	−0.049	−0.012
η	0.202	0.569	0.387	0.58
U	0.341	0.060	0.213	0.020
V	−0.430	−0.005	−0.065	−0.001
W	0.225	0.006	0.023	0.003
No of reflections	640	602	410	562
No of refined parameters	37	37	37	37
Space group	*Pnma*	*Pnma*	*Pnma*	*Pnma*
a (Å)	7.524(8)	7.526(2)	7.463(6)	7.401(5)
b (Å)	6.574(7)	6.574(8)	6.462(9)	6.375(6)
c (Å)	7.450(1)	7.451(8)	7.351(1)	7.235(2)
V (Å^3)	368.6	368.7	354.6	341.4
Z	4	4	4	4
R_F	0.026	0.026	0.025	0.029
R_B	0.040	0.038	0.035	0.041
R_P	0.036	0.081	0.060	0.080
R_{WP}	0.047	0.123	0.082	0.116
CR_P	0.076	0.092	0.07	0.098
CR_{WP}	0.088	0.138	0.09	0.135
χ^2	0.18	2.72	4.34	2.22

Table 2
Atomic coordinates and isotropic temperature factors (BVS: Bond valence sum)

Atom	Site	Sym.	X	y	z	$B_{iso.}$ (Å^2)	BVS	Occ.
$LiTiOAsO_4$ (XRD)								
Ti	4*c*	m	0.333(5)	0.750	0.225(6)	0.14(3)		1
Li	4*a*	$\bar{1}$	0.000	0.000	0.000	0.53(6)		1
As	4*c*	m	0.374(7)	0.250	0.130(2)	0.31(2)		1
O(1)	4*c*	m	0.117(3)	0.750	0.159(2)	0.52(8)		1
O(2)	4*c*	m	0.806(9)	0.750	0.002(1)	0.88(2)		1
O(3)	4*c*	m	0.063(2)	0.250	0.490(2)	1.14(6)		1
O(4)	8*d*	1	0.873(1)	0.453(9)	0.233(2)	0.03(1)		1
$LiTiOAsO_4$ (neutrons)								
Ti	4*c*	m	0.334(6)	0.750	0.226(1)	0.26(2)	4.18	1
Li	4*a*	$\bar{1}$	0.000	0.000	0.000	1.11(5)	1.00	1
As	4*c*	m	0.374(3)	0.250	0.130(1)	0.36(9)	5.02	1
O(1)	4*c*	m	0.116(4)	0.750	0.163(3)	0.71(5)	1.89	1
O(2)	4*c*	m	0.808(3)	0.750	−0.001(1)	0.52(6)	2.08	1
O(3)	4*c*	m	0.063(1)	0.250	0.491(3)	0.89(1)	2.03	1
O(4)	8*d*	1	0.872(9)	0.454(5)	0.236(1)	0.62(1)	2.1	1
$LiTiOAs_{0.5}P_{0.5}O_4$ (XRD)								
Ti	4*c*	m	0.332(3)	0.750	0.222(4)	0.44(5)	4.23	1
Li	4*a*	$\bar{1}$	0.000	0.000	0.000	0.45(4)	1.08	1
P	4*c*	m	0.374(7)	0.250	0.131(4)	0.51(9)	4.77	0.5
As	4*c*	m	0.374(7)	0.250	0.131(4)	0.51(9)	4.77	0.5
O(1)	4*c*	m	0.113(5)	0.750	0.153(5)	0.14(5)	1.93	1
O(2)	4*c*	m	0.798(6)	0.750	0.000	0.22(4)	2.04	1
O(3)	4*c*	m	0.055(6)	0.250	0.488(2)	0.48(6)	2.01	1
O(4)	8*d*	1	0.872(6)	0.453(9)	0.234(3)	0.26(1)	2.05	1
$LiTiOPO_4$ (XRD)								
Ti	4*c*	m	0.322(1)	0.750	0.219(7)	0.64(2)	4.2	1
Li	4*a*	$\bar{1}$	0.000	0.000	0.000	0.95(3)	1.02	1
P	4*c*	m	0.374(3)	0.250	0.127(6)	0.63(2)	4.87	1
O(1)	4*c*	m	0.112(1)	0.750	0.150(4)	0.61(4)	2	1
O(2)	4*c*	m	0.791(7)	0.750	−0.001(7)	0.61(4)	1.99	1
O(3)	4*c*	m	0.047(7)	0.250	0.484(2)	0.61(4)	2.02	1
O(4)	8*d*	1	0.871(5)	0.446(1)	0.247(9)	0.61(4)	2.04	1

3. Results and discussion

3.1. Structure refinement of $LiTiOAs_{1-x}P_xO_4$ ($0 \leqslant x \leqslant 1$)

The structure of $LiTiOAs_{1-x}P_xO_4$ ($x = 0$, 0.5 and 1) has been refined with the Rietveld method using the Fullprof program [15]. The initial atomic coordinates used for the refinement were those given by Robertson et al. [3] and the calculations were performed in the *Pnma* space group. After the refinement of 37 parameters (fractional atomic coordinates, temperature factors, scale factor, zero point, unit cell parameters, background terms and profile parameters), values of Bragg's coefficient obtained for $LiTiOAsO_4$ and $LiTiOPO_4$, respectively ($R_B = 0.038$ and 0.041) were lower than those given by other authors (0.139 and 0.175) [3]. This result is, probably, due to the purity of $LiTiOAsO_4$ and $LiTiOPO_4$ phases prepared at low temperature (600 and 800 °C, respectively). Refinement of the structure of $LiTiOAsO_4$ using neutron diffraction was done to confirm the distribution of Li in 4*a* site. The results are quite similar to those obtained by X-ray diffraction. An excellent fit of calculated and observed X-ray and neutrons powder diffraction was achieved (Figs. 1 and 2). Details of the final refinement are given in Table 1. The atomic parameters are shown in Table 2. The selected bond lengths are listed in Table 3. Calculated valences ($S_i = \Sigma \exp[(R_{ij} - d_{ij})/b]$ with $b = 0.37$ Å) based on bond strength analysis [16] are in good agreement with the expected formal oxidation states of As^{5+}, P^{5+}, Ti^{4+}, Li^{+} and O^{2-} (Table 2).

Table 3
Selected interatomic distances (Å) for $LiTiOAs_{1-x}P_xO_4$ ($x = 0$, 0.5 and 1)

	$LiTiOAsO_4$	$LiTiOAs_{0.5}P_{0.5}O_4$	$LiTiOPO_4$
X–O(2)	1.685(8)	1.614(1)	1.529(7)
X–O(3)	1.679(4)	1.611(6)	1.516(6)
X–O(4) × 2	1.683(3)	1.647(1)	1.540(4)
Ti–O(1)	1.700(9)	1.709(4)	1.704(2)
Ti–O(1)	2.301(7)	2.289(2)	2.275(4)
Ti–O(2)	2.038(7)	2.056(1)	2.061(8)
Ti–O(3)	1.918(3)	1.914(1)	1.922(5)
Ti–O(4) × 2	1.993(1)	1.963(1)	1.974(2)
Li–O(1) × 2	2.211(4)	2.145(3)	2.100(5)
Li–O(2) × 2	2.193(9)	2.207(1)	2.217(8)
Li–O(4) × 2	2.004(6)	1.990(1)	2.058(9)

The structure of $LiTiOAs_{1-x}P_xO_4$ ($0 \leqslant x \leqslant 1$) (Fig. 3) consists of a 3D network of TiO_6 octahedra and XO_4 ($X = As_{1-x}P_x$) tetrahedra sharing corners. In this framework there are octahedral cavities occupied by lithium atoms. XO_4 tetrahedra share one corner (O4) with LiO_6 octahedron and three corners (O2, O3, O4) with three different TiO_6 octahedra. LiO_6 octahedra share faces with TiO_6 octahedra. XO_4 ($X = As_{1-x}P_x$) tetrahedra are isolated, however, TiO_6 octahedra are linked together by corners and form infinite chains along *a*-axis. These chains are linked together in a three-dimensional network by corners of XO_4 tetrahedra (Fig. 4). Titanium atoms are

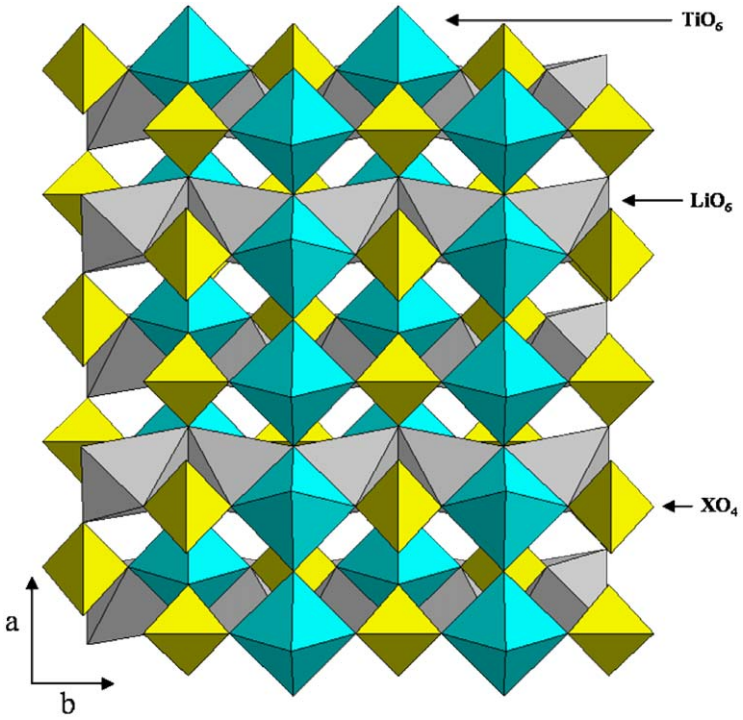

Fig. 3. Structure of $LiTiOXO_4$ ($X = As_{1-x}P_x$).

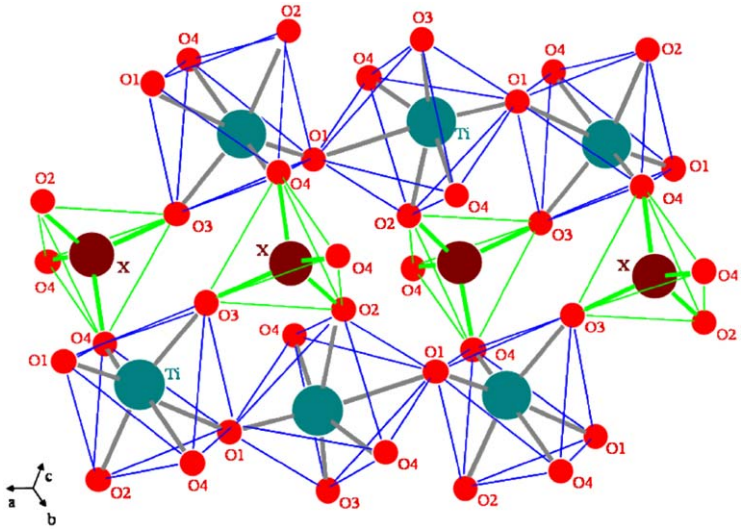

Fig. 4. –Ti–O–Ti– chains in $LiTiOXO_4$ ($X = As_{1-x}P_x$) compounds.

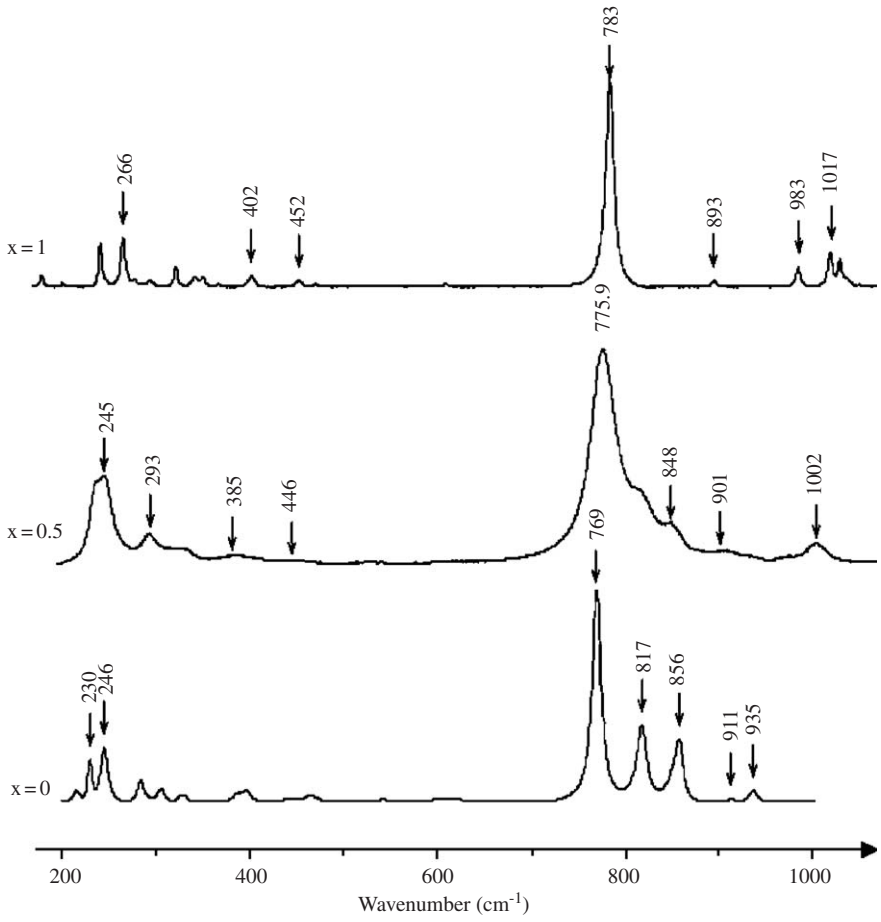

Fig. 5. Raman spectra of $LiTiOAs_{1-x}P_xO_4$ ($x = 0$, 0.5 and 1).

displaced from the geometrical centre of the octahedra resulting in alternating of short ($\approx$1.700 Å) and long (2.300–2.275 Å) Ti–O bonds. O1TiO1 angles in –Ti–O–Ti– chains increase systematically as P is replaced by As [$LiTiOPO_4$:172.7°, $LiTiOAs_{0.5}P_{0.5}O_4$:173.7°, $LiTiOAsO_4$:175°]. This straightening of chain presumably results from

the O1 atoms being forced further apart by the larger AsO_4 tetrahedra. The four remaining Ti–O bond distances have intermediate values ranging between 1.914 and 2.060 Å.

The Li atom is coordinated to six oxygen atoms with distances ranging from 1.990 to 2.211 Å, the sum of the ionic radii is 2.220 Å [17]. LiO_6 polyhedra, located between –Ti–O–Ti– chains, share two faces with each TiO_6 octahedron. Every LiO_6 polyhedron is connected to another LiO_6 by common edge (O1–O2) and form chains running parallel to *b*-axis.

3.2. Vibrational spectroscopy

Vibrational analysis for an isolated XO_4^{3-} (X = As, P) anion with point group Td leads to 4 modes: $A_1[(\nu_1;\nu_s(XO_4)]$, $E[(\nu_2;\ \delta_s(XO_4)]$ and $2F_2[\nu_3;\ \nu_{as}(XO_4)$ and $\nu_4;\ \delta_{as}(XO_4)]$. All of them are Raman-active modes whereas only ν_3 and ν_4 are IR-active modes. By means of separation of the vibrations in the crystalline state into internal and external modes, a factor group analysis of XO_4^{3-} (X = As, P) has been performed using the C_s symmetry. Thus, for the stretching vibrations we can expect 8 Raman-active modes: $[A_g + B_{3g}](\nu_1)$, $[2A_g + B_{1g} + B_{2g} + 2B_{3g}](\nu_3)$ and 7 IR-active modes: $[B_{1u} + B_{2u}](\nu_1)$, $[2B_{1u} + 2B_{2u} + B_{3u}](\nu_3)$. For the bending vibrations we achieved 10 Raman-active modes: $[A_g + B_{1g} + B_{2g} + B_{3g}](\nu_2)$, $[2A_g + B_{1g} + B_{2g} + 2B_{3g}](\nu_4)$ and 8 IR-active modes: $[B_{1u} + B_{2u} + B_{3u}](\nu_2)$, $[2B_{1u} + 2B_{2u} + B_{3u}](\nu_4)$. The external modes consist of the translational modes of the Li^+, Ti^{4+} and XO_4^{3-} (X = As, P) ions.

Figs. 5 and 6 compare Raman and IR spectra of $LiTiOAs_{1-x}P_xO_4$ ($0 \leqslant x \leqslant 1$), respectively. In previous Raman studies of $NaZr_2(AsO_4)_3$, $Na_3CaTi(PO_4)_3$, $Na_3MgTi(PO_4)_3$ and $Na_5Ti(PO_4)_3$, in which XO_4 (X = P, As) tetrahedra as AO_6 (A = Zr, Ti) octahedra are isolated from each other, no band is observed in 700–800 cm^{-1} region [18–21]. Then, the strong band situated at $\approx 775\,cm^{-1}$ in the Raman spectra of $LiTiOAs_{1-x}P_xO_4$ ($0 \leqslant x \leqslant 1$) (observed at $\approx 820\,cm^{-1}$ in IR spectra), can not be attributed to the X–O (X = P, As) or to the A–O (A = Zr, Ti) vibrations. On the other hand, its frequency is slightly influenced by the composition. Consequently, it is exclusively correlated to Ti–O vibration in –Ti–O–Ti– chains.

The high frequency part (800–1100 cm^{-1}) of the Raman spectra of $LiTiOAs_{1-x}P_xO_4$ ($0 \leqslant x \leqslant 1$) exhibits 4 bands for $LiTiOAsO_4$, 5 bands for $LiTiOAs_{0.5}P_{0.5}O_4$ and 6 bands for $LiTiOPO_4$. The IR spectrum of $LiTiOAsO_4$ exhibits 6 bands or shoulders. Eight and 4 bands are shown for $LiTiOAs_{0.5}P_{0.5}O_4$ and $LiTiOPO_4$, respectively (Table 4). All of these bands correspond to the stretching vibration of the X–O bonds in XO_4 (X = As, P) tetrahedra in good

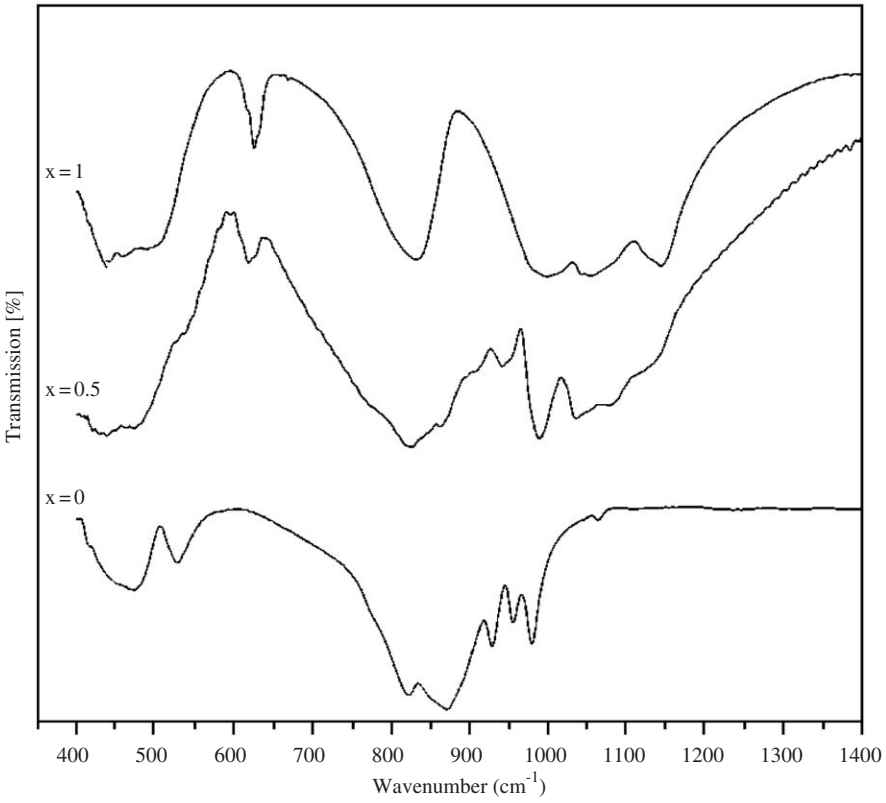

Fig. 6. Mid-infrared spectra of $LiTiOAs_{1-x}P_xO_4$ (x = 0, 0.5 and 1).

Table 4
Vibrational modes of $LiTiO(As_{1-x}P_xO_4)$ ($x = 0$, 0.5 and 1) (sh: shoulder)

Raman			IR			Assignment
$X = 0$	$x = 0.5$	$x = 1$	$X = 0$	$x = 0.5$	$x = 1$	
		1047				Stretching vibrations of X–O (X = As, P) bonds
		1034		1130	1142	
		1026		1078		
	1002	1017	1064		1054	
	973	983		1037	1041	
935			979	988	997	
911				975(sh)		
	901		956	942		
		893	929	908(sh)		
856	848					
817	813		872	863		
			850(sh)			
769	776	783	823	827	832	Ti–O vibrations
610		608		621	625	Bending vibration
541					617(sh)	
493			528	536(sh)		
465		468			495	
449	446	452	472	472		
396		402	449		458	
388	385			437	441	
		366	415			
		349				
		343				External modes
328	330	322				
306						
284	293	294				
		277				
246	247	266				
	243					
230	237	242				
216						

agreement with the results of the factor group analysis. With replacement of arsenic with phosphorus in the crystalline unit ($LiTiOAsO_4$), the surrounding of the X–O bonds is changed and in addition to the broadening of the bands ($LiTiOAs_{0.5}P_{0.5}O_4$), a shift of the modes to higher wavenumbers takes place ($LiTiOPO_4$). This displacement of the peaks towards the high energy in $LiTiOPO_4$ phosphate is due to smaller P–O (≈ 1.53 Å) bonds compared to As–O (≈ 1.683 Å) bonds. A similar behaviour has been previously observed for $NaZr_2(AsO_4)_3$ and $NaZr_2(PO_4)_3$ [18]. The additional bands appear in Raman (901, 973 and 1002 cm^{-1}) and in IR (988, 1037 and 1130 cm^{-1}) spectra of $LiTiOAs_{0.5}P_{0.5}O_4$ and become more intense in $LiTiOPO_4$. These new bands are assigned to the P–O stretching vibrations. The X–O bending vibrations are to be found in the region of 400–700 cm^{-1} with 10 Raman-active bands and 8 IR-active bands for the compounds with factor group *Pnma*. For $LiTiOAsO_4$ and $LiTiOPO_4$ we find 7 and 6 bands, respectively, of the predicted 10 Raman bands but in the IR spectra only 4 bands are visible in this range. The external modes appear in the low region of the spectra consist of the translation modes of the Li^+, Ti^{4+} and XO_4^{3-} ions.

3.3. Crystallochemical study

X-ray diffraction patterns of $LiTiOAs_{1-x}P_xO_4$ ($0 \leqslant x \leqslant 1$) (Fig. 7) were indexed in the orthorhombic system with *Pnma* space group. A solid solution $LiTiOAs_{1-x}P_xO_4$ has been obtained in the whole composition range explored: $0 \leqslant x \leqslant 1$. With replacement of arsenic with phosphorus, a shift of peaks toward higher values of 2θ Bragg's angles takes place. Simultaneously, new peaks appear (i.e. 0 1 1, 2 0 0, 1 0 2, 1 0 2). The cell parameters variations as a function of x are given in Fig. 8. The progressive substitution of arsenic by phosphorus provokes a decrease of a, b and c parameters. This decrease is in favor of the occupation of 4c sites by the P^{5+} ions ($rP^{5+} = 0.17$ Å) of

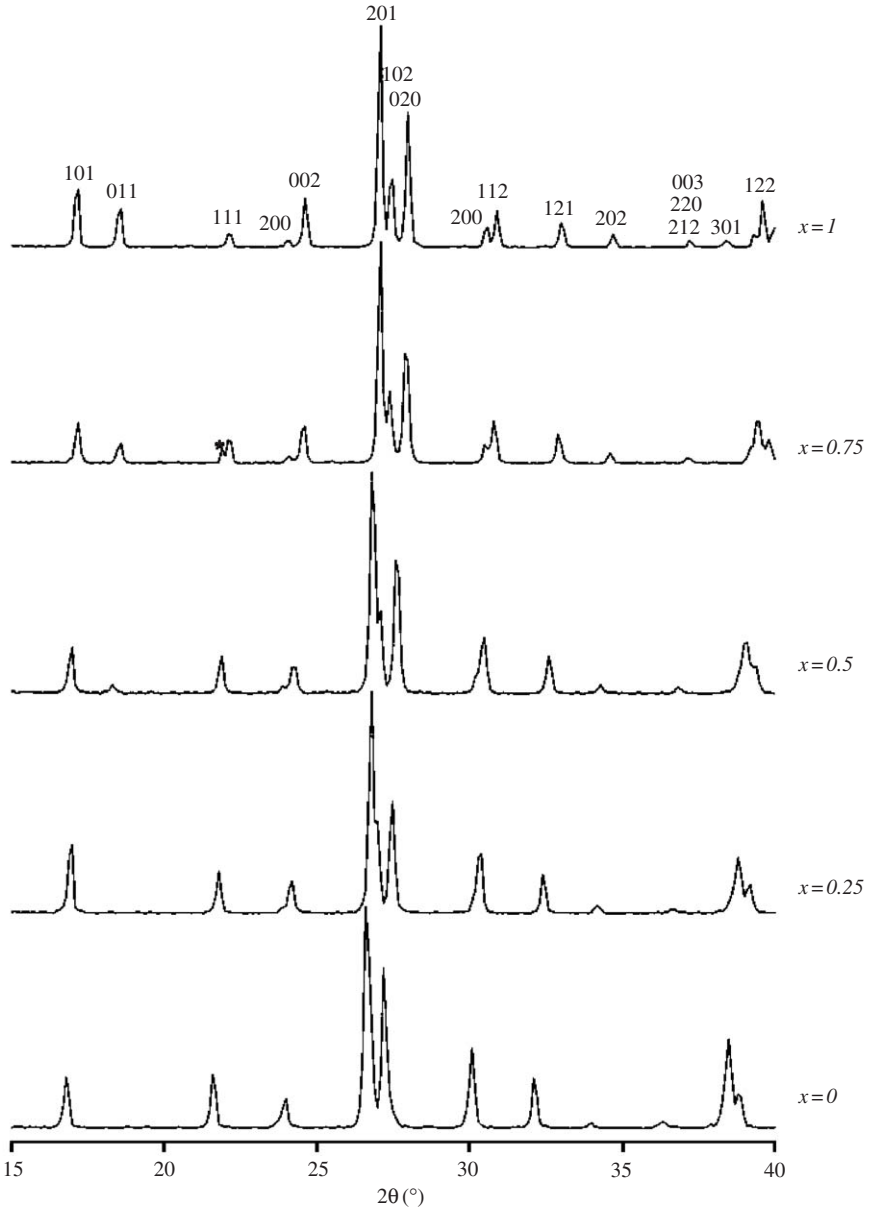

Fig. 7. X-ray powder patterns of $LiTiOAs_{1-x}P_xO_4$ ($0 \leqslant x \leqslant 1$) (*non-indexed pic).

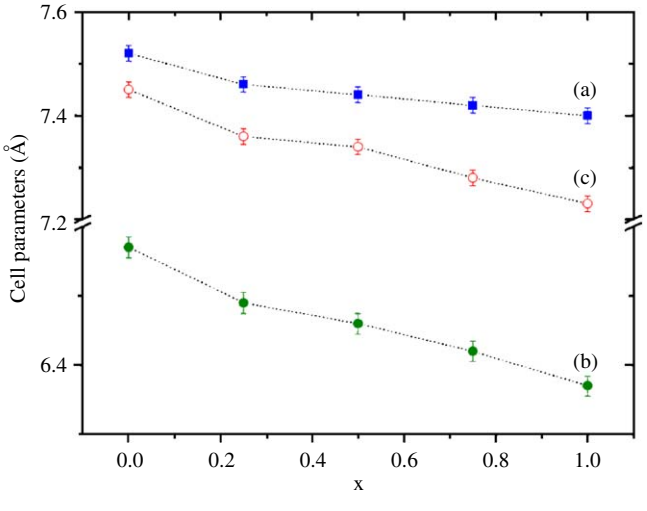

Fig. 8. Cell parameters evolution versus composition for $LiTiOAs_{1-x}P_xO_4$ ($0 \leqslant x \leqslant 1$) compounds.

size smaller than the As^{5+} one ($rAs^{5+} = 0.33$ Å) [17]. As previously discussed in detail, the structure of $LiTiOAs_{1-x}P_xO_4$ ($0 \leqslant x \leqslant 1$) is formed by 3D network of TiO_6 octahedra and XO_4 ($X = As_{1-x}P_x$) tetrahedra sharing corners. When X is As, As/P and P, the lengths of O–O tetrahedron edges is $\approx$2.7, $\approx$2.6 and $\approx$2.5 Å, respectively. Consequently, the cell parameters of $LiTiOAsO_4$ are superior to those of $LiTiOPO_4$.

3.4. Thermal stability of $LiTiOAsO_4$

Room temperature X-ray diffraction patterns of $LiTiOAsO_4$ prepared in Platinum crucible at different temperatures between 200 and 1000 °C are given in Fig. 9. $LiTiOAsO_4$ prepared by the method described previously is amorphous at 200 °C. At 400 °C, XRD analysis shows a mixture of phases ($LiTiOAsO_4$, TiO_2 anatase, $Li_4Ti_5O_{12}$ and other extra peaks). At 600 °C

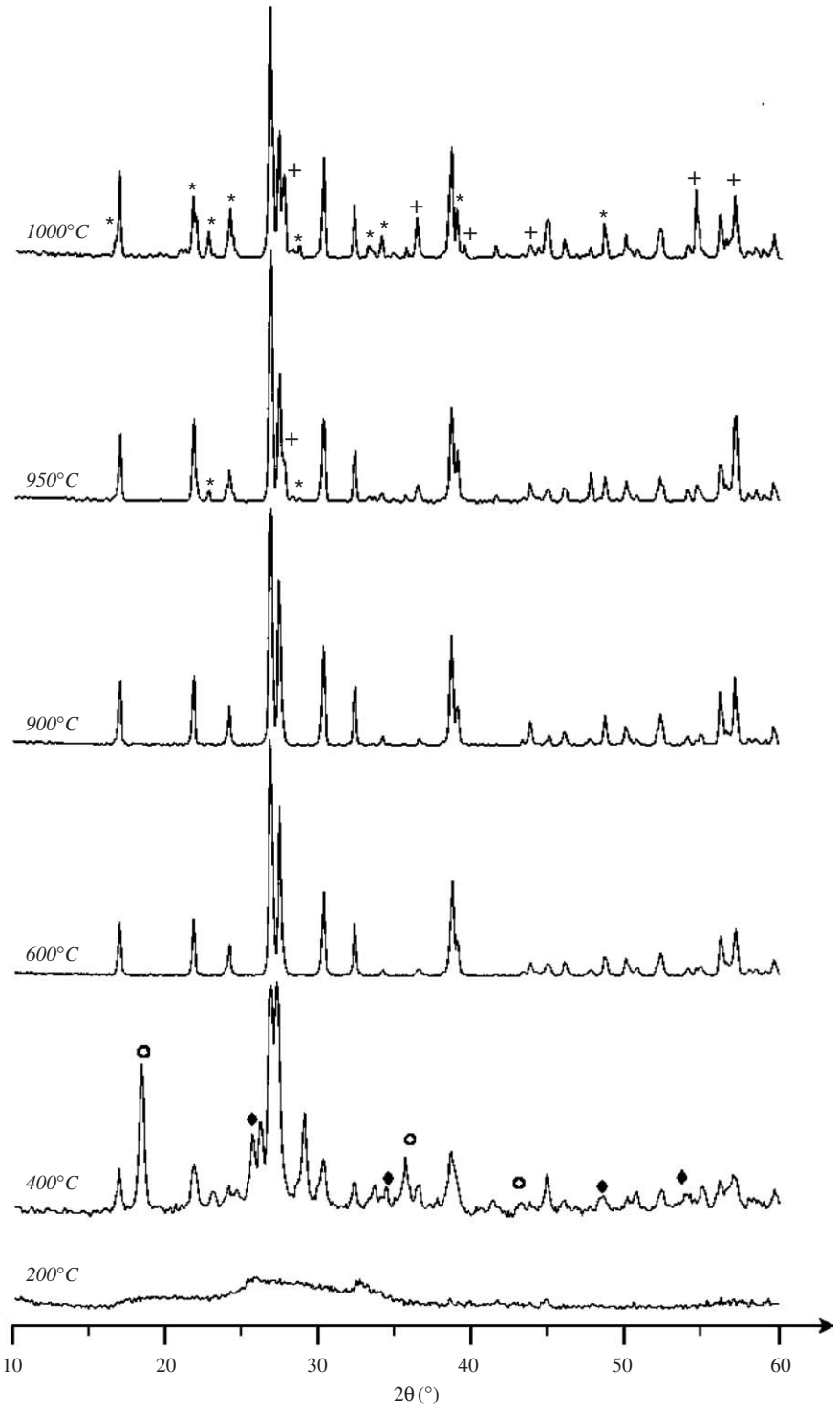

Fig. 9. X-ray patterns recorded at room temperature for $LiTiOAsO_4$, heated at different temperatures in platinum crucible. [(+) TiO_2 rutile, (♦) TiO_2 anatase, (○) $Li_4Ti_5O_{12}$, (*) Li_3AsO_4].

only $LiTiOAsO_4$ is present. After 900 °C $LiTiOAsO_4$ began to loss weight. The X-ray pattern shows the presence of $LiTiOAsO_4$, Li_3AsO_4 and TiO_2 rutile. As can be seen from the Li_2O–TiO_2–As_2O_5 ternary diagram (Fig. 10), we can deduce that the decomposition of $LiTiOAsO_4$ is accompanied by the loss of As_2O_5 according to the scheme:

$$3LiTiOAsO_4 \rightarrow 3TiO_2 + LiAsO_4 + \overrightarrow{As_2O_5}.$$

When $LiTiOAsO_4$ is heated at high temperature in alumina crucible, X-ray pattern reveals the presence of $AlAsO_4$,

TiO_2 rutile and Li_3AsO_4 (Fig. 11). We can then deduce that $LiTiOAsO_4$ reacts with the crucible (Al_2O_3) according to the reaction:

$$3LiTiOAsO_4 + Al_2O_3(\text{Crucible}) \rightarrow 3TiO_2 + Li_3AsO_4 + 2AlAsO_4$$

This reaction was confirmed by action of 3 mol of $LiTiOAsO_4$ with 1 mol of Al_2O_3 (powder) at 950 °C. XRD pattern shows the presence of TiO_2, Li_3AsO_4 and $AlAsO_4$.

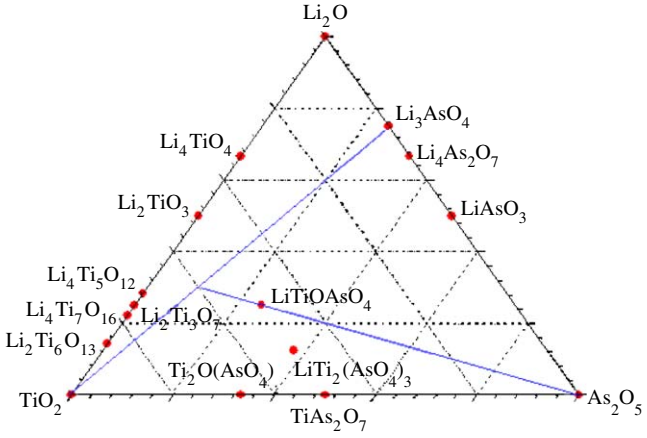

Fig. 10. Ternary diagram of Li_2O–TiO_2–As_2O_5 system.

4. Conclusion

Polycrystalline samples of $LiTiOAs_{1-x}P_xO_4$ ($0 \leqslant x \leqslant 1$) have been prepared and characterized by X-ray diffraction, Raman and IR spectroscopy. Their structure has been determined on powder by Rietveld method. It is formed by infinite chains of distorted corners-sharing TiO_6 octahedra linked together via XO_4 (X = As, P) tetrahedra. This study shows the existence of a solid solution in the domain $0 \leqslant x \leqslant 1$. Cell parameter variation results mainly from the size of X^{5+} (X = As, P) ions. Assignments of internal modes of XO_4 (X = As, P) tetrahedra have been made. The number of peaks observed, in Raman and IR spectra is in good agreement with that predicted by the factor group analysis of *Pnma* space group.

References

[1] I. Tordjman, R. Masse, J.C. Guitel, Z. Kristallogr. 139 (1974) 103.
[2] R. Masse, J.C. Grenier, Bull. Soc. Fr. Minéral. Cristallogr. 94 (1971) 437.
[3] A. Robertson, J.G. Fletcher, J.M.S. Skakle, A.R. West, J. Solid State Chem. 109 (1994) 53.
[4] S.C. Mayo, P.A. Thomas, S.J. Teat, G.M. Loiacono, D.N. Loiacono, Acta Cryst. B 50 (39) (1994) 655.
[5] J. Protas, G. Marnier, B. Boulanger, B. Menaert, Acta Cryst. C 45 (39) (1989) 1123.
[6] M. Pierrou, F. Laurell, H. Karlsson, T. Kellner, C. Czeranowsky, G. Huber, Opt. Lett. 24 (1999) 205.
[7] P.A. Thomas, S.C. Mayo, B.E. Watts, Acta Cryst. B 48 (39) (1992) 401.
[8] M. Kunz, R. Dinnebier, L.K. Cheng, E.M. McCarron, D.E. Cox, J.B. Parise, M. Gehrke, J. Calabrese, P.W. Stephens, T. Vogt, R. Papoular, J. Solid State Chem. 120 (1995) 299.

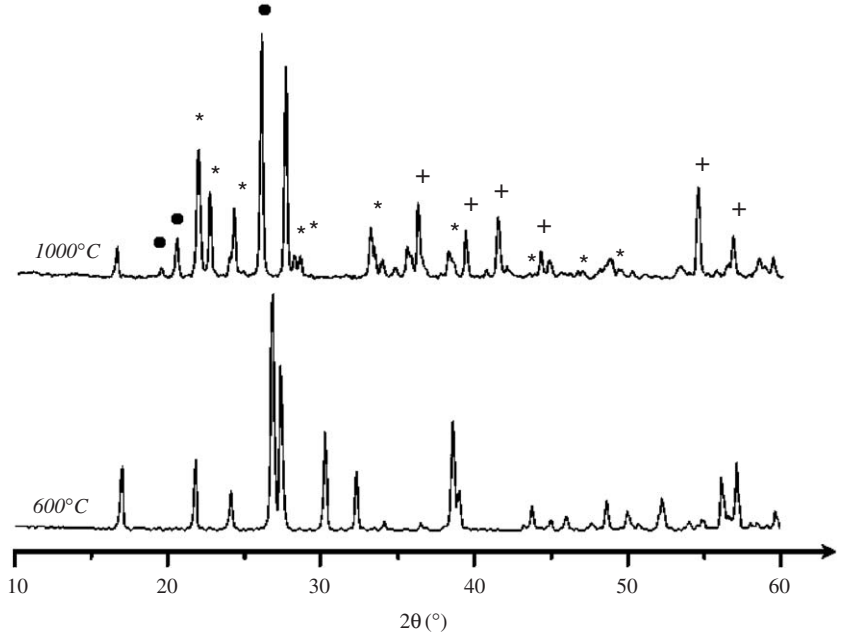

Fig. 11. X-ray diffraction pattern of $LiTiOAsO_4$ prepared in Al crucible (600 °C: $LiTiOAsO_4$; 1000 °C: (*) Li_3AsO_4 (+) TiO_2 (●) $AlAsO_4$).

[9] R.V. Pisarev, R. Farhi, P. Moch, V.I. Voronkova, Condens. J. Phys. Mater. 2 (1990) 7555.
[10] P.G. Nagornoy, A.A. Kapshuck, N.V. Stus, N.S. Slobodyanik, A.N. Chernega, Russ. J. Inorg. Chem. 36 (11) (1991) 1551.
[11] P. Gravereau, J.P. Chaminade, B. Manoun, S. Krimi, A. El Jazouli, Powder Diffr. 14 (1999) 10.
[12] H. Belmal, Thesis, University Hassan II—Mohammedia, Morocco, 2004.
[13] B. Manoun, A. El Jazouli, P. Gravereau, J.P. Chaminade, Mater. Res. Bull. 40 (2005) 229.
[14] B. Manoun, A. El Jazouli, P. Gravereau, J.P. Chaminade, J.C. Grenier, Ann. Chim. Sci. Mater. 25 (Suppl. 1) (2000) 71.
[15] J. Rodriguez-Carvajal, Collected Abstract of Powder Diffraction Meeting, Toulouse, France, 1990, pp. 127.
[16] N.E. Brese, M. O'Keeffe, Acta. Crystallogr. B 47 (1991) 192.
[17] R.D. Shannon, Acta Crystallogr. A 32 (1976) 751.
[18] M. Chakir, A. El Jazouli, D. de Waal, Mater. Res. Bull. 38 (2003) 1773.
[19] S. Krimi, A. El Jazouli, A. Lachgar, L. Rabardel, D. de Waal, J.R. Ramos-Barrado, Ann. Chim. Sci. Mater. 25 (Suppl. 1) (2000) 75.
[20] S. Krimi, A. El Jazouli, D. de Waal, J.R. Ramos-Barrado, In: Proceedings of the Sixth ESG Conference, Montpellier, 2–6 June 2002.
[21] S. Krimi, I. Mansouri, A. El Jazouli, J.P. Chaminade, P. Gravereau, G. Le Flem, J. Solid State Chem. 105 (1993) 561.